



Preparation and characterization of microfiltration membrane based on polyethylene terephthalate nanofibrous support

Mohsen Moslehi¹ · Abbas akbarzadeh²

Received: 2 August 2023 / Revised: 8 November 2023 / Accepted: 10 November 2023 /
Published online: 23 December 2023

© The Author(s), under exclusive licence to Springer-Verlag GmbH Germany, part of Springer Nature 2023

Abstract

The new class of microfiltration (MF) membranes based on nanofibrous sub-layers was investigated in this study. To this end, polyethylene terephthalate (PET) nanofibrous layers were produced via electrospinning technique based on PET supports as baking material, and subsequently, the solvent vapor treatment was applied for pore size modification of nanofibrous membranes. Capillary flow porometry and scanning electron microscopy were used to evaluate of pore size and morphology of the membranes, respectively. Moreover, filtration performance was evaluated by water flux and microparticle/bacteria retention. The results showed that average pore size of PET electrospun nanofibrous membrane was greatly reduced from 1.2 to 0.4 μm during modification process. Solvent vapor-treated MF membranes show significantly higher flux and acceptable rejection compared to commercial MF membranes.

Keywords Microfiltration · Electrospinning · Solvent vapor treatment · Polyethylene terephthalate

Introduction

Population increments and the requirement for water resources are one of the main concerns in the world. According to reports, nearly 1 billion people are in a deficit of clean water [1, 2]. Membrane technology is a cost-effective and practical technique applied in the filtration of pollutants from water. The pressure-driven membrane

✉ Abbas akbarzadeh
abbasakbarzadeh@yahoo.com; a.akbarzadeh@wri.ac.ir

Mohsen Moslehi
m.moslehi@chem.ui.ac.ir; M.moslehi91@gmail.com

¹ Department of Nanotechnology, Faculty of Chemistry, University of Isfahan, Isfahan, Iran

² Water and Wastewater Research Center (WWRC), Water Research Institute, Tehran, Iran

filtration processes are categorized into microfiltration (MF), ultrafiltration (UF), nanofiltration (NF), and reverse osmosis (RO) [3]. Microfiltration membranes with the lowest energy-consuming and rapid filtration rate are mostly applied in the separation of contaminants such as microparticles in the different industry application [4]. Commercial MF membranes are produced based on phase inversion from solution or melt casting techniques, and these processes need high exactitude control of production conditions, also commercial membranes, having higher density and fast clogging [5].

Nanofiber is one of the nanotechnology outputs, widely used in different areas such as air purification [6], tissue science [7], and liquid phase filtration including MF [8], UF [9], NF [10, 11], and RO [12] membranes. Due to the higher porosity, interconnected pore, large surface area, and easier controllable producing condition, nanofibrous membranes are interesting among researchers for the production of a new class of liquid phase membranes [13]. The electrospinning technique is used to prepare nanofibrous membranes. In this method, a high electric force between two poles caused the formation of nanofiber jets. Subsequently, by the evaporation and elimination of solvent from the jets, nanofiber and then nanofibrous mats were formed. The process can be controlled by adjusting the solution and environment conditions [14]. Controlled pore size nanofibrous MF membranes have been manufactured by altering the electrospinning condition, physical and chemical treatment of nanofibrous mats. Wang et al. prepared polyacrylonitrile (PAN) nanofibrous MF membranes with a uniform structure by controlling of electrospinning parameters [15]. Hsiao et al. demonstrated the potential of polyvinyl alcohol (PVA) nanofibrous mat for MF membrane, which could be prepared by crosslinking with glutaraldehyde (GA) [16]. In our previous work, microfiltration membranes with a pore size of 0.2–0.47 μm were prepared with a controlled interfacial polymerization technique, based on polyurethane nanofibrous supports [17].

PET is a thermoplastic polymer with wide industrial applications that includes a wide range of properties like elastomeric, hydrolytic resistance, and nanofibrous support characteristics [18, 19]. In this study, the solvent vapor treatment method was used to modify the nanofibrous membranes. At the following, in the first step, PET nanofibrous supports were prepared by electrospinning technique, and after optimization of the solution and process, solvent vapor treatment was applied for modification and controlling the membrane pore size. In the end, the modified membranes were characterized by SEM, capillary flow porometry, water flux, and MF retention methods.

Experimental

Materials

PET granule was prepared from Tondgooyan Petrochemical Industries Co., Iran. Nonwoven PET (Hollytex 3242) was prepared by Ahlstrom Mount Holly Springs, USA. Trifluoroacetic acid (TFA), dichloromethane (DCM) and LiCl were purchased from Sigma-Aldrich Co. Polybead carboxylate microparticles (0.20, 0.50, and

1.0 μm) were purchased from Polysciences, Inc. Commercial membranes (Model GSWP, Millipore, 0.45 and 0.22 μm) were purchased for comparison.

PET nanofibrous membranes

A solution of 18% wt PET was prepared in TFA/DCM (80/20 v/v) and stirred till completely dissolved. LiCl was added as an electrospinning additive. The prepared solution was placed in a syringe possessing 10 ml and 0.7 mm nozzle diameter, and then the electrospinning was performed under the conditions listed in Table 1, on the PET substrate support layer.

Due to the same material of the nanofibers and the substrate, and the presence of residual solvent in the nanofiber jets during electrospinning, the adhesion of the nanofibers to the substrate was done well, and this is an advantage in making membranes with resistance to delamination.

Modification of nanofibrous membranes

For pore size modification, PET nanofibrous membranes were put in a chamber saturated with solvent (DCM) vapor. In this way, the membranes were placed inside the chamber for different periods of time, and in the following, the effect of the solvent vapor and the treatment time on these membranes were investigated.

Characterization

The morphology of all membranes was investigated by scanning electron microscopy (SEM). The average fiber diameter of PET/PET nanofibrous membranes was assigned by the SEM image analyzer software.

The porosity of PET nanofibrous membranes is determined from Eq. (1) [19].

$$\text{Porosity} = [1 - (\rho' / \rho)] \times 100\% \quad (1)$$

where ρ' and ρ present the apparent density and bulk density of the PET nanofibrous membranes, respectively. In order to calculate apparent density, samples of about 5 cm^2 and $150 \pm 14 \mu\text{m}$ were weighted. The bulk density of PET was taken at 1.4 g/cm^3 .

Table 1 Electrospinning conditions

Polymer concentration (wt%)	18
TFA/DCM(v/v)	80/20
LiCl (wt%)	0.01
Solution flow rate (ml/h)	0.8
Applied voltage (kV)	30
Distance between needle and collector (cm)	14
Drum collector speed (rpm)	800

The bubble point and mean pore size of the PET nanofibrous membranes were evaluated by capillary flow porometry technique [20].

In this test, the wet and dry membranes were placed in a holder, and the changes in airflow with pressure were drawn for each sample, as shown in Fig. 1a. For wet samples, the membrane surface is entirely soaked in the wetting agent (alcohol with a surface tension of 23 dyn/cm) and, with a gradual increase in pressure, the airflow is plotted. At the following, the dry membrane is put inside the cell, and the airflow is measured and the flow diagram of the dry sample is plotted. In the end, the dry air flow values against the pressure are halved, and the diagram of half-dry airflow is plotted beside the wet flow. So, the plots intersect each other at a specific point. The corresponding pressure of the wet flow starting and the intersection of wet flow and half-dry flow are assigned and placed in Eq. (2) which is calculated as the bubble point and the average hole size, respectively.

$$D = 2860\gamma \cos \theta / p \quad (2)$$

D , θ , p , and γ are the pore diameter membrane (μm), contact angle of wetting agent, pressure (Pa), and surface tension of the wetting agent (dyn/cm), respectively.

For evaluation of MF membrane performance (rejection and flux), the homemade dead-end filtration set-up was applied (Fig. 1b). The microparticle retention of the MF membranes was measured based on the following procedure. 200 ppm aqueous suspensions of polybead microparticles in different sizes were prepared by ultrasonic dispersion, and subsequently, the 30 cc of the solution was filtered through the filtration system (PET/PET nanofibrous and commercial GSWP membranes). The carbon concentrations in the primary and permeate solution were measured with a total organic carbon analyzer (TOC, Shimadzu TOC-VCPN). The rejection of the carboxylate microparticles is calculated based on Eq. (3):

$$R = [1 - (C_p/C_f)] \times 100 \quad (3)$$

C_f and C_p show the carbon concentration in primary and permeate solution.

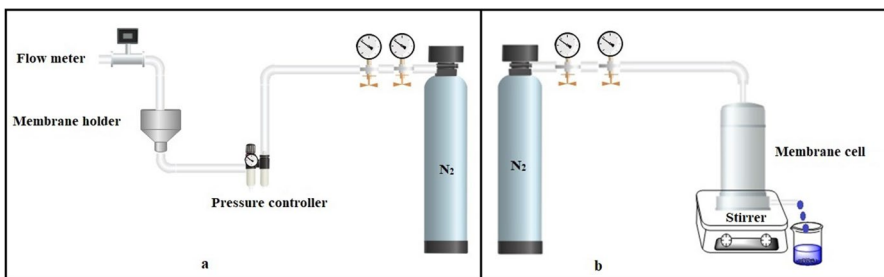


Fig. 1 Schematic diagram of the capillary flow porometer set-up **a** and MF test set-up **b**

Results and discussion

Morphological study of PET nanofibrous membranes

The SEM technique was used to evaluate the morphology of nanofibrous PET membranes. As shown in Fig. 2a–d, the PET nanofibrous membrane produced from 18 wt% in 80/20 v/v TFA/DCM had a non-uniform structure and film-like morphology with an average fiber diameter of 200 ± 30 nm. Surface tension is one of the important parameters that effect on nanofibrous membranes morphology. The higher surface tension of solution brings the lower elongation of the nanofibrous jet in the electrical field. As a result, the polymeric solution droplets cannot be sufficiently elongated in the electrical field, and consequently, some beads and film-like structures are produced [21].

For improving nanofibrous membrane structure, various parameters such as additives, solution components, electrical fields, and surrounding conditions have been evaluated in various literature [22]. In this study, LiCl was applied as an additive for electrospinning of PET nanofibrous membrane with uniform structure. LiCl induces higher conductivity for polymeric solution and as a result, electrical force dominates on surface tension of the solution, and then more stretching force is performed in the electrical field. Consequently, polymeric jets are more stretched and the beaded and film-like structures. Figure 2e–h shows the SEM images of PET nanofibrous membranes that were prepared from the same polymeric solution composition in the presence of LiCl as an additive. As seen from the images, no beaded and film-like structure was detected for them.

In the next step, after optimization of the nanofibrous supporting layer, solvent vapor treatment was applied to modify and reduce nanofibrous membrane pores (Table 2).

Figure 3 demonstrates the SEM images of the solvent-treated nanofibrous membranes. In this modification, samples were placed in a solvent vapor chamber for different periods of time. Figure 3a, b is related to pristine nanofibrous membranes

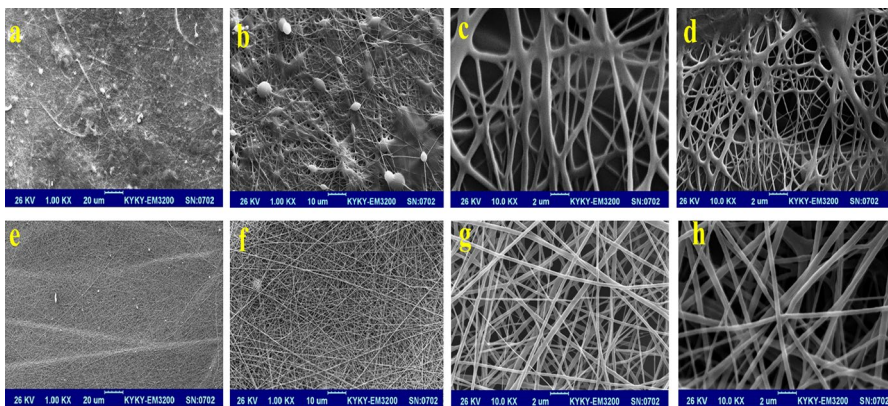
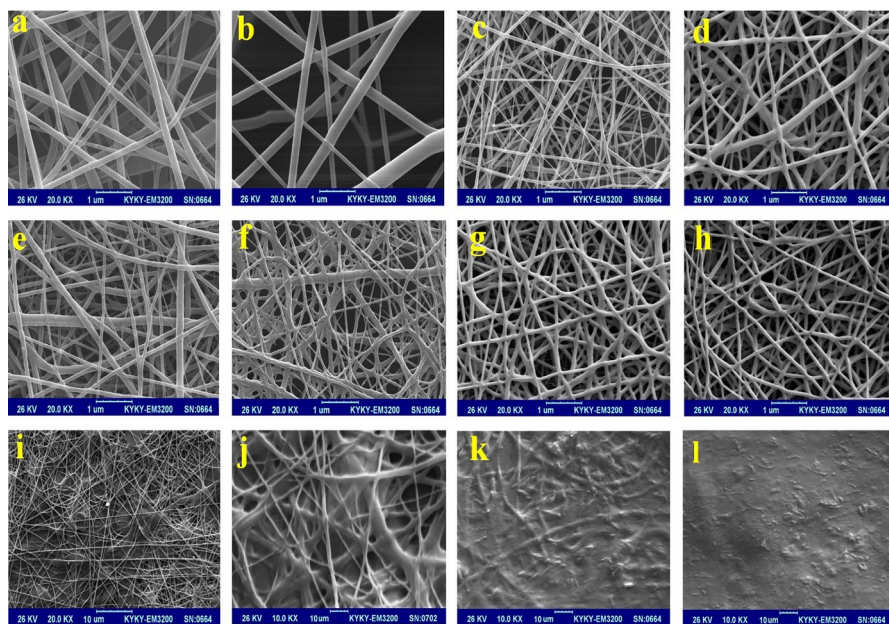


Fig. 2 SEM images of PET (18% (w/v) a–d) and PET (18% (w/v), LiCl 0.01 wt%) e–h) membranes

Table 2 Solvent vapor method for membrane modification

Membrane no	Solvent	Time (s)
M ₁	DCM	0
M ₂	DCM	30
M ₃	DCM	60
M ₄	DCM	120
M ₅	DCM	180
M ₆	DCM	240
M ₇	DCM	300

**Fig. 3** SEM images of modified PET nanofibrous membranes under different modification conditions

(M₁). Figure 3c, d shows the morphology of M₂ membranes. After the 30 s exposing membranes in the chamber, small changes have been made in the morphology of the membrane. In the case of M₃, the samples were placed in the chamber for the 60 s. As seen from Fig. 3e, f, the morphology of the nanofiber was changed, and the interconnecting of nanofiber was slightly increased. For M₄, the exposing time was increased to 120 s, and the morphology of the nanofibrous network changed more. As seen from Fig. 3g, h, due to swelling, the diameter of the nanofiber was increased and also the interconnecting of the nanofiber improved. Figure 3i, j is related to M₅ that the time of vapor solvent treatment was 180 s. As seen from the image, the swelling and interconnecting of nanofiber was more improved, and the morphology was changed from nanofiber to nanofiber-film structure.

By increasing solvent vapor treating time to 240 s, M_6 in this case, the morphology of the surface has changed significantly, so that the film structure is dominant to the structure of the fibers while maintaining the lucidity of nanofiber morphology (Fig. 3k). For M_7 , the treating time was enhanced to 300 s. As seen from Fig. 3l, by increasing solvent vapor exposure, the solvent penetration, swelling, and local dissolution of fiber result in the total abolishing of the nanofiber morphology and film structure formation. As a result, the surface pores of M_6 and M_7 membranes are reduced to such an extent that the size of the pores is out of the area of microfiltration. Hence, according to image analyses, pore size characteristics of M_1 to M_5 were investigated.

Porometry evaluation of PET/PET nanofibrous membranes

A home-designed capillary flow porometry (based on ASTM-F316 03) was used to analyze the pore characteristic of samples. Alcohol (aqueous isopropyl alcohol 70 wt%) with a surface tension of 27.48 dynes/cm at 25 °C was applied as the wetting agent. Table 3 shows the results of dry flow, wet flow, and half-dry flow data for PET/PET nanofibrous membranes.

As seen from the results, the bubble point and mean flow pore size of the pristine membrane (M_1) are 8.7 and 1.6 μm , respectively. For M_2 , the bubble point and mean flow pore size were reduced slightly. As mentioned early, no clear change in morphology was observed for the M_2 membrane. In the case of M_3 , the largest pore and mean pore size were reduced to 3.5 and 1.1 μm , respectively. In this way, by enhancement of treating time to 120 s, the largest pore and mean pore size of M_4 were reduced to 1.2 and 0.43 μm , respectively, and for M_5 with a treatment time of 180 s, the bubble point and mean pore size of this sample reached to 0.9 and 0.26 μm , respectively.

Microfiltration test

The PET/PET nanofibrous membranes with a total thickness of $150 \pm 14 \mu\text{m}$ and commercial membranes (CMs, 0.45 and 0.22 μm GSWP, Millipore) with a thickness of $150 \pm 10 \mu\text{m}$ were investigated by MF filtration set-up. Prior to the experiment, all

Table 3 Capillary flow porometry results for PET/PET nanofibrous membranes

Membrane no	Intersection of wet and half-dry flow pressure (bar)	Wet flow starting pressure (bar)	Mean pore diameter (μm)	Largest pore–bubble point (μm)
M_1	0.49	0.09	1.6	8.7
M_2	0.51	0.09	1.5	8.5
M_3	1.1	0.22	0.7	3.5
M_4	1.75	0.65	0.43	1.2
M_5	3.02	0.87	0.26	0.9

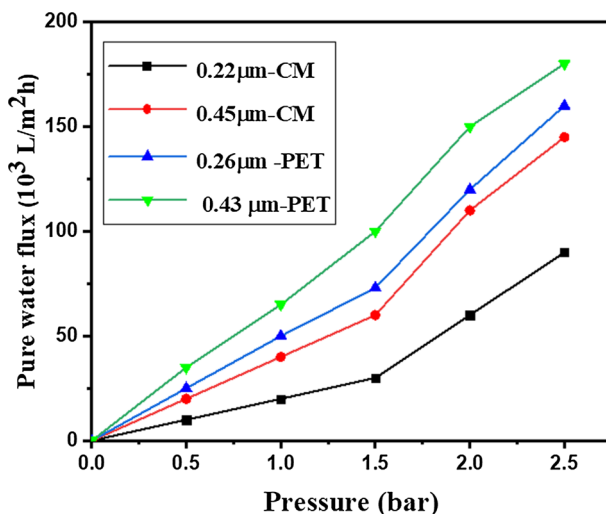


Fig. 4 Pure water flux for electrospun PET/PET and commercial membranes (CMs)

Table 4 Rejection of microparticle standard test marker using for electrospun and commercial membranes

Microparticle size	0.2 μm (%)	0.5 μm (%)	1 μm (%)
PET/PET ENM (0.43 μm)	90 ± 3	97.5 ± 2	98 ± 0.2
PET/PET ENM (0.26 μm)	97 ± 1	98 ± 1	99 ± 0.4
GSWP, Millipore (0.45 μm)	90 ± 1	97 ± 1	99 ± 0.3
GSWP, Millipore (0.22 μm)	99 ± 0.3	99 ± 0.1	99 ± 0.5

of the samples were compressed at 1 bar with water. Figure 4 shows the pure water flux of nanofibrous and commercial membranes.

Due to the open pore structure and high porosity of PET/PET nanofibrous membranes, the pure water flux is two times higher flux than the commercial membranes in distinct pressures. To study the filtration performance of the electrospun nanofibrous membranes, standard microparticles were applied as the test markers. Due to the spherical shape of polymeric particles, this experiment could be a criterion of membrane pores diameter. As shown in Table 4, the electrospun membranes and commercial membranes, showed a similar rejection ratio on 1.0, 0.50, and 0.2 μm particles. Two types of membranes have the same mean pore size, so the MF efficiency of membranes in microparticle retention is comparable.

Conclusion

The solvent vapor treatment strategy was utilized to modify and adjust PET/PET electrospun MF membrane pore size. It was implied that this method can prominently the pore size of PET nanofibers. In this work, at first, the optimum condition

for electrospinning parameters on the corresponding nanofiber structure was systematically evaluated. In the following, for altering pore size, the solvent vapor method was applied. In this experiment, the effect of exposure time was investigated. In the end, the microfiltration performance of nanofibrous and commercial membranes was investigated. The results showed that the nanofibrous MF membrane presented significantly higher flux performance (2 times) over the commercial membranes having the same mean flow pore size.

References

1. Hwang L, Waage S, Stewart E, Morrison J, Gleick, P H, Morikawa M (2007) At the crest of a wave: a proactive approach to corporate water strategy. BSR (Business for Social Responsibility) and Pacific Institute
2. Dolan F, Lamontagne J, Link R, Hejazi M, Reed P, Edmonds J (2021) Evaluating the economic impact of water scarcity in a changing world. *Nat Commun* 12(1):1915
3. Van der Bruggen B, Vandecasteele C, Van Gestel T, Doyen W, Leysen R (2003) A review of pressure-driven membrane processes in wastewater treatment and drinking water production. *Environ Prog* 22(1):46–56
4. Anis SF, Hashaikeh R, Hilal N (2019) Microfiltration membrane processes: A review of research trends over the past decade. *Water Process Eng* 32:100941
5. Gul A, Hruza J, Yalcinkaya F (2021) Fouling and chemical cleaning of microfiltration membranes: a mini-review. *Polymers* 13(6):846
6. Lyu C, Zhao P, Xie J, Dong S, Liu J, Rao C, Fu J (2021) Electrospinning of nanofibrous membrane and its applications in air filtration: A review. *Nanomaterials* 11(6):1501
7. Tanzli E, Ehrmann A (2021) Electrospun nanofibrous membranes for tissue engineering and cell growth. *Appl Sci* 11(15):6929
8. Moslehi M, Mahdavi H (2020) Preparation and characterization of electrospun polyurethane nanofibrous microfiltration membrane. *Polym Environ* 28:2691–2701
9. Hezarjaribi M, Bakeri G, Sillanpää M, Chaichi MJ, Akbari S, Rahimpour A (2021) Novel adsorptive PVC nanofibrous/thiol-functionalized TNT composite UF membranes for effective dynamic removal of heavy metal ions. *Environ Manag* 284:111996
10. Moslehi M, Mahdavi H, Ghaffari A (2021) Preparation and characterization of polyamide thin film composite nanofiltration membrane based on polyurethane nanofibrous support. *Polym Environ* 29:463–2477
11. Mahdavi H, Moslehi M (2016) A new thin film composite nanofiltration membrane based on PET nanofiber support and polyamide top layer: preparation and characterization. *Polym Res* 23:1–9
12. Kim S, Heath DE, Kentish SE (2020) Composite membranes with nanofibrous cross-hatched supports for reverse osmosis desalination. *ACS Appl Mater Interfaces* 12(40):44720–44730
13. Kaur S, Sundarajan S, Rana D, Sridhar R, Gopal R, Matsuura T, Ramakrishna S (2014) The characterization of electrospun nanofibrous liquid filtration membranes. *Mater Sci* 49:6143–6159
14. Li Y, Zhu J, Cheng H, Li G, Cho H, Jiang M, Zhang X (2021) Developments of advanced electrospinning techniques: a critical review. *Adv Mater Technol* 6(11):2100410
15. Wang R, Liu Y, Li B, Hsiao BS, Chu B (2012) Electrospun nanofibrous membranes for high flux microfiltration. *Membr Sci* 392:167–174
16. Liu Y, Wang R, Ma H, Hsiao BS, Chu B (2013) High-flux microfiltration filters based on electrospun polyvinylalcohol nanofibrous membranes. *Polymer* 54(2):548–556
17. Moslehi M, Mahdavi H (2019) Controlled pore size nanofibrous microfiltration membrane via multi-step interfacial polymerization: preparation and characterization. *Sec. Purif Technol* 223:96–106
18. Hao J, Lei G, Li Z, Wu L, Xiao Q, Li W (2013) A novel polyethylene terephthalate nonwoven separator based on electrospinning technique for lithium-ion battery. *Membr Sci* 428:11–16
19. Ma Z, Kotaki M, Yong T, He W, Ramakrishna S (2005) Surface engineering of electrospun polyethylene terephthalate (PET) nanofibers towards development of a new material for blood vessel engineering. *Biomaterials* 26(15):2527–2536

20. American Society for Testing and Materials, (2003) Standard test methods for pore size characteristics of membrane filters by bubble point and mean flow pore test, West Conshohocken, PA: ASTM
21. Huan S, Liu G, Han G, Cheng W, Fu Z, Wu Q, Wang Q (2015) Effect of experimental parameters on morphological, mechanical and hydrophobic properties of electrospun polystyrene fibers. *Materials* 8(5):2718–2734
22. Cui J, Li F, Wang Y, Zhang Q, Ma W, Huang C (2020) Electrospun nanofiber membranes for wastewater treatment applications. *Sep Purif Technol* 250:117116

Publisher's Note Springer Nature remains neutral with regard to jurisdictional claims in published maps and institutional affiliations.

Springer Nature or its licensor (e.g. a society or other partner) holds exclusive rights to this article under a publishing agreement with the author(s) or other rightsholder(s); author self-archiving of the accepted manuscript version of this article is solely governed by the terms of such publishing agreement and applicable law.